

**STUDY ON THE EFFECTS OF *Catharanthus roseus*-
SILVER NANOPARTICLES ON HUMAN
HEPATOCELLULAR CARCINOMA CELL LINE
HEPG2**

NUR ASNA BINTI AZHAR

UNIVERSITI SAINS MALAYSIA

2024

**STUDY ON THE EFFECTS OF *Catharanthus roseus*-
SILVER NANOPARTICLES ON HUMAN
HEPATOCELLULAR CARCINOMA CELL LINE
HEPG2**

by

NUR ASNA BINTI AZHAR

**Thesis submitted in fulfilment of the requirements
for the degree of
Doctor of Philosophy**

September 2024

ACKNOWLEDGEMENT

بِسْمِ اللَّهِ الرَّحْمَنِ الرَّحِيمِ

First and foremost, praise to Allah S.W.T, the Almighty for the successful completion of this dissertation. This dissertation would not have been possible without the help of so many people in so many ways. I would like to express my deepest appreciation to my supervisor, Dr Nor Hazwani binti Ahmad, who has supported me throughout my period of study with her knowledge, persistent guidance and courage. Without her support, I would not have the opportunity to gain valuable knowledge and experiences. I would like to acknowledge the technical expertise of the laboratory staff. In addition, thank you to all the staffs from animal laboratory for their assistance. I am thankful to my lab mate Aishah binti Abu Bakar that had been together with me throughout this journey. I am grateful for the great memories that we had together. My deepest gratitude goes to my parents Azhar bin Hasan and Rosidah binti Haroon for their endless love and encouragement. Thank you so much to my siblings Azzah, Azri, Azni, and Azim for their emotional support. I am grateful to my husband, Mohd Zamir Bin Zainol Abidin, for his patience, understanding, and unwavering support. Lastly, I offer my regards and blessings to all of those who supported me in any respect during the completion of the study. Thank you.

TABLE OF CONTENTS

ACKNOWLEDGEMENT	ii
TABLE OF CONTENTS	iii
LIST OF TABLES	x
LIST OF FIGURES	xii
LIST OF ABBREVIATIONS	xxiv
LIST OF UNITS	xxix
LIST OF SYMBOLS	xxxii
LIST OF APPENDICES	xxxiii
ABSTRAK	xxxiii
ABSTRACT	xxxvi
CHAPTER 1 INTRODUCTION	1
1.1 Background	1
1.2 Rationale of study.....	4
1.3 Research objectives	8
CHAPTER 2 LITERATURE REVIEW	11
2.1 Cancer	11
2.1.1 Global cancer statistics.....	12
2.1.2 Cancer statistics in Malaysia	13
2.1.3 Hepatocellular carcinoma.....	15
2.2 Nanotechnology	16
2.2.1 Introduction	16
2.2.2 Biomedical Application of Nanomaterials.....	17
2.2.3 Clinically approved nanoparticles	19
2.3 Silver Nanoparticles (AgNPs).....	22
2.3.1 Introduction	22

2.3.2	Patent analysis of AgNPs in cancer therapy.....	23
2.3.3	Synthesis of AgNPs	24
2.3.3(a)	Physical and chemical methods	25
2.3.3(b)	Biological methods.....	29
2.3.4	Characterisation of AgNPs.....	38
2.3.4(a)	Ultraviolet-Visible spectroscopy (UV–Vis)	38
2.3.4(b)	Fourier transform infrared (FTIR) spectroscopy.	40
2.3.4(c)	Transmission electron microscopy (TEM).....	40
2.3.4(d)	Scanning electron microscopy (SEM).....	41
2.3.4(e)	X-ray diffraction (XRD).....	42
2.3.4(f)	Particle size and zeta potential analysis	43
2.3.5	Cellular uptake of AgNPs.....	45
2.3.5(a)	Cell membrane interactions and AgNPs entry into the cell	45
2.3.5(b)	The physicochemical properties of AgNPs affect their cellular uptake.....	50
2.4	<i>Catharanthus roseus</i> (L) G. Don (<i>C. roseus</i>).....	53
2.5	Mechanism of cell death.....	58
2.5.1	Type I cell death	58
2.5.1(a)	Death-receptor-induced apoptotic pathway(extrinsic).....	58
2.5.1(b)	Mitochondrial-mediated apoptotic pathway (Intrinsic)	59
2.5.1(c)	Other signalling pathways mediated to apoptosis.....	63
CHAPTER 3 MATERIALS AND METHOD.....		67
3.1	Materials and reagents	67
3.2	Preparation of <i>C. roseus</i> -AgNPs	70
3.2.1	<i>C. roseus</i> aqueous extraction	70
3.2.2	Synthesis of <i>C. roseus</i> -AgNPs.....	70

3.2.3	Preparation of camptothecin.....	71
3.3	Preparation of Cells	71
3.3.1	Cell Lines	71
3.3.1(a)	Cell thawing.....	72
3.3.1(b)	Passaging cells	73
3.3.1(c)	Cell counting.....	73
3.3.1(d)	Cryopreservation.....	74
3.4	Antiproliferative effects of <i>C. roseus</i> -AgNPs.....	74
3.4.1	Cell Viability Assay	74
3.4.2	Selectivity Index (SI)	75
3.4.3	IncuCyte® Morphological Observation.....	75
3.4.4	Statistical analysis.....	75
3.5	Oxidative stress effects of HepG2 cells treated with <i>C. roseus</i> -AgNPs.....	76
3.5.1	Nitric oxide (NO) release assay	76
3.5.1(a)	Griess reagent calibration	76
3.5.2	Reactive oxygen species (ROS) assay	77
3.5.3	Intracellular calcium measurement.....	78
3.5.4	Mitochondrial membrane potential ($\Delta\psi_m$) assay	78
3.5.5	Statistical analysis.....	79
3.6	The cell death mechanism of HepG2 cells lines treated with <i>C. roseus</i> -AgNPs	80
3.6.1	Caspase 3/7 and 8 activities.....	80
3.6.2	Caspase 9 activity	80
3.6.3	Annexin V-FITC/PI staining assay	81
3.6.4	Cell cycle analysis.....	82
3.6.5	Comet assay	83
3.6.5(a)	Qualitative analysis of comet assay	83
3.6.5(b)	Quantitative analysis of comet assay	84

3.6.6	Statistical analysis	84
3.7	Cellular uptake of <i>C. roseus</i> -AgNPs in HepG2 cells	85
3.7.1	Quantification of <i>C. roseus</i> -AgNPs cellular uptake.	85
3.7.2	Quantification of <i>C. roseus</i> -AgNPs exocytosis	85
3.7.3	Selective inhibition of <i>C. roseus</i> -AgNPs uptake	86
3.7.4	Visualisation of <i>C. roseus</i> -AgNPs uptake	87
3.7.5	Statistical analysis	87
3.8	Transcriptomic profiling of HepG2 treated with <i>C. roseus</i> -AgNPs.....	88
3.8.1	Total RNA extraction and sample quality check.....	88
3.8.2	Beijing Genomics Institute sequencing.....	88
CHAPTER 4 RESULTS		90
4.1	Anti-proliferative effects <i>C. roseus</i> -AgNPs.....	90
4.1.1	Anti-proliferative effects of <i>C. roseus</i> -AgNPs on HepG2 cells	90
4.1.2	Anti-proliferative effects of <i>C. roseus</i> aqueous extract on HepG2 cells	92
4.1.3	Anti-proliferative effects of camptothecin on HepG2 cells	94
4.1.4	Anti-proliferative effects of <i>C. roseus</i> -AgNPs on THLE-3 cells	96
4.1.5	Anti-Proliferative effects of <i>C. roseus</i> aqueous extract on THLE-3 cells	98
4.1.6	Anti-proliferative effects of camptothecin on THLE-3 Cells.....	100
4.1.7	IC ₅₀ Summary	102
4.1.8	Selectivity Index (SI)	104
4.1.9	IncuCyte® Morphological Observation.....	106
	4.1.9(a) Morphology of HepG2 at 24, 48, and 70 hours of incubation	106
	4.1.9(b) Morphology of THLE-3 at 24, 48 and 70 hours of incubation	110
4.2	The oxidative stress effect of <i>C. roseus</i> -AgNPs towards HepG2 cells	114

4.2.1	Nitric oxide (NO) release assay	114
4.2.2	Intracellular reactive oxygen species (ROS) assay	116
4.2.3	Quantification of intracellular Ca ²⁺	118
4.2.4	<i>C. roseus</i> -AgNPs induced mitochondrial damage in HepG2	122
4.2.4(a)	Quantitative analysis of HepG2 mitochondrial membrane potential	122
4.2.4(b)	Qualitative analysis of mitochondrial membrane potential in HepG2	124
4.3	The cell death mechanism of HepG2 cells treated with <i>C. roseus</i> -AgNPs. .	126
4.3.1	Activation of executioner and effector caspases	126
4.3.1(a)	Activation of caspase 8.....	126
4.3.1(b)	Activation of caspase 9.....	128
4.3.1(c)	Activation of caspase 3/7.....	130
4.3.2	Detection of early and late apoptosis of HepG2 cells treated with <i>C. roseus</i> -AgNPs.....	132
4.3.3	Effects of <i>C. roseus</i> -AgNPs on the HepG2 cells cycle.....	136
4.3.4	Effects of <i>C. roseus</i> -AgNPs on the HepG2 cells DNA damage.	141
4.4	Cellular uptake of <i>C. roseus</i> -AgNPs in HepG2 cells	144
4.4.1	Quantification of intracellular Ag.....	144
4.4.2	Exocytosis of <i>C. roseus</i> -AgNPs	146
4.4.3	Endocytosis vs Exocytosis of <i>C. roseus</i> -AgNPs	148
4.4.4	Selective inhibition of <i>C. roseus</i> -AgNPs uptake pathways.....	150
4.4.5	Visualisation <i>C. roseus</i> -AgNPs uptake	155
4.5	Transcriptomic profiling of HepG2 cells treated with <i>C. roseus</i> -AgNPs.....	159
4.5.1	Quantitative and qualitative measurement of total RNA	159
4.5.2	Sequencing data filtering.....	161
4.5.3	Genome mapping	165
4.5.4	SNP and INDEL detection	165

4.5.5	Differentially splicing gene detection	169
4.5.6	Gene expression analysis.....	171
4.5.6(a)	Gene mapping and expression	171
4.5.6(b)	Sequencing saturation, reads coverage, distribution analysis transcripts, and correlation between samples	172
4.5.6(c)	Differentially Expressed Gene (DEG) detection	174
4.5.6(d)	<i>C. roseus</i> -AgNPs exposure altered the expression multiple genes in HepG2 cells.....	176
4.5.6(e)	Pathway analysis of DEG.....	185
CHAPTER 5 DISCUSSION		188
5.1	<i>C. roseus</i> -AgNPs induced anti-proliferative effects on HepG2 cells.....	190
5.2	<i>C. roseus</i> -AgNPs induced oxidative stress and mitochondrial depolarisation in HepG2 cells.....	195
5.3	<i>C. roseus</i> -AgNPs induced apoptosis in the HepG2 cells.....	201
5.4	<i>C. roseus</i> -AgNPs entered HepG2 cells via endocytosis.....	207
5.5	<i>C. roseus</i> -AgNPs dysregulated gene and biological pathways.....	214
5.5.1	mRNA transcriptome analysis identified 296 protein-coding genes.....	214
5.5.2	<i>C. roseus</i> -AgNPs induced the expression of stress-associated genes.....	217
5.5.3	<i>C. roseus</i> -AgNPs increased the expression of tumour suppressor genes and apoptotic genes.....	218
5.5.4	<i>C. roseus</i> -AgNPs activated signal transduction pathway such as mitogen-activated protein kinase (MAPK) signalling pathway	219
5.5.5	<i>C. roseus</i> -AgNPs activated Tumour Necrosis Factor (TNF) signalling pathway	220
5.5.6	<i>C. roseus</i> -AgNPs elicited the activation of TGF- β signalling pathway	222
5.5.7	The uptake of <i>C. roseus</i> -AgNPs occurred via endocytosis.	222
5.5.8	The uptake of <i>C. roseus</i> -AgNPs caused cell cycle arrest.....	225

CHAPTER 6 CONCLUSION AND FUTURE RECOMMENDATION	228
6.1 Conclusion	228
6.2 Study limitations and future recommendations.....	230
REFERENCES	233
APPENDICES	
LIST OF PUBLICATIONS AND AWARDS	

LIST OF TABLES

	Page
Table 2.1	Commonly used nanomaterials in biomedicine for various applications. Taken from Barkalina <i>et al.</i> (2014)..... 18
Table 2.2	Clinically approved intravenous nanoparticle therapies and diagnostics, grouped by their broad indication. Taken from Anselmo &Mitragotri (2016) 21
Table 2.3	Synthesis of AgNPs by physical methods. Taken from Venditto <i>et al.</i> (2010)..... 27
Table 2.4	Synthesis of AgNPs by chemical methods. Taken from Venditto <i>et al.</i> (2010)..... 28
Table 2.5	Bacteria-, fungi-mediated synthesis of AgNPs. Taken from Venditto <i>et. al</i> (2010)..... 36
Table 2.6	Plant-mediated synthesis of AgNPs. Taken from Venditto <i>et al.</i> (2010)..... 37
Table 3.1	List of reagents 67
Table 3.2	List of solvents and chemical 68
Table 3.3	List of materials 68
Table 3.4	Characteristics of <i>C. roseus</i> -AgNPs that had done previously by Ghozali <i>et al.</i> , 2018..... 71
Table 4.1	The IC ₅₀ Summary 103
Table 4.2	The selectivity index..... 105
Table 4.3	Dot plots of flow cytometry analysis of treated HepG2 cells for 24, 48, and 72 hours. Annexin-V stained HepG2 cells_ FITC/PI staining and analysed using flow cytometry. 135
Table 4.4	Fluorescence microscope image at 10× magnification of apoptotic inducing effect on HepG2 cells assessed by comet assay..... 143

Table 4.5	Clean reads quality metrics	163
Table 4.6	Summary of genome mapping	165
Table 4.7	SNP variant type summary.....	166
Table 4.8	Summary of gene mapping ratio	171
Table 4.10	The significant KEGG pathways.....	186

LIST OF FIGURES

	Page
Figure 2.1	Estimated number of new cases worldwide in 2020. Taken from http://gco.iarc.fr 13
Figure 2.2	Number of new cases and the top common cancer in Malaysia in 2022. Taken from http://gco.iarc.fr 14
Figure 2.3	The patent documents related to AgNPs in cancer therapy that were published, filed, and granted over the years. Taken from Lens.org .. 24
Figure 2.4	AgNPs synthesis top-down approach and bottom-up approach. Taken from Xu <i>et al.</i> (2020)..... 24
Figure 2.5	UV-Vis absorption spectrum of (a) cannonball leaf extract and (b) biosynthesised AgNPs. Taken from Devaraj <i>et al.</i> (2013) 40
Figure 2.6	Example of XRD patterns of AgNPs synthesised using <i>Catharanthus roseus</i> leaf extract. Taken from Ghozali <i>et al.</i> (2015)..... 43
Figure 2.7	Example of Zeta potential patterns of AgNPs synthesised using <i>Catharanthus roseus</i> leaf extract. Taken from Mukunthan <i>et al.</i> (2011)..... 44
Figure 2.8	Schematic illustration of the opsonisation process, initiated by the adsorption of immunoglobulins or other complement proteins (opsonin) to the AgNPs surface. Opsonised particles are subsequently identified through receptors on phagocytic cells and internalised. Taken from Yamamura <i>et al.</i> (2018). 47
Figure 2.9	Entry of AgNPs into cells using different endocytotic pathways. (a) Macropinocytosis and phagocytosis. (b) Clathrin-mediated endocytosis, clathrin-caveolin independent endocytosis and caveolae-mediated endocytosis. Taken from Foroozandeh <i>et al.</i> (2018)..... 50

Figure 2.10	Various species of <i>C. roseus</i> . Photographs of eight varieties of <i>C. roseus</i> . (a) Patricia White (PW); (b) First Kiss Polka Dot (FKD); (c) First Kiss Peach (FKP); (d) Experimental Rose Pink (ER); (e) Experimental Deep Pink (ED); (f) Cooler Orchid (CO); (g) Victory Red (VR); (h) Blue Pearl (BP). Taken from (Malaysia Biodiversity Centre, 2013).....	54
Figure 2.12	Death-receptor-mediated (extrinsic) is initiated at the cellular membrane through the binding of death receptor ligand to their respective receptor ligands and mitochondrial-mediated (intrinsic) apoptotic pathways involved with the mitochondria. Both pathways lead to caspase activation and cleavage of specific cellular substrates. Taken from Hu <i>et al.</i> (2003).....	60
Figure 3.1	This flowchart summarises the study's methodology, including five main experimental phases: (1) Antiproliferative effects are assessed through cell viability assays, IC ₅₀ determination, selectivity index (SI), and IncuCyte morphological observations. (2) Oxidative stress effects was evaluated using nitric oxide (NO) release assays, reactive oxygen species (ROS) assays, intracellular calcium measurements, and mitochondrial membrane potential ($\Delta\Psi_m$) assays. (3) The cell death mechanism is investigated by measuring caspase 3/7, 8, and 9 activities, performing Annexin V-FITC/PI staining, cell cycle analysis, and comet assays. (4) Cellular uptake and exocytosis of <i>C. roseus</i> -AgNPs are quantified, including selective inhibition studies and visualisation of nanoparticle uptake. (5) RNA analysis involves total RNA extraction, quantitative and qualitative measurement, library construction, bioinformatics workflow, and identification of targeted expressed genes.	69
Figure 3.2	Visual classification suggested by Collins <i>et al.</i> (1997)Images of comets (from lymphocytes) stained with DAPI. They represent class 0 (no damage), class 1 (low damage), class 2 (moderate damage), class 3 (high damage), class 4 (severe damage) as used for visual scoring. Taken from Collins <i>et al.</i> (1997).	84

- Figure 4.1 (A) The cytotoxicity of HepG2 cells lines treated with different concentrations of *C. roseus*-AgNPs, while untreated HepG2 cells and AgNO₃ treatment represent control. (B) The line graph showed the IC₅₀ of HepG2 cells treated with *C. roseus*-AgNP. Data are presented as mean±SD, n=3. Comparisons between treatment and untreated were done using one-way ANOVA, followed by the Dunnet post-test for (* $p<0.05$; ** $p<0.01$; *** $p<0.001$). 91
- Figure 4.2 (A) The cytotoxicity of HepG2 cells lines treated with different concentrations of *C. roseus* aqueous extract, while untreated HepG2 cells and AgNO₃ treatment represent control. (B) The line graph showed the IC₅₀ of *C. roseus* aqueous extract treated HepG2 cells. Data are presented as mean±SD, n=3. Comparisons between treatment and untreated were done using one-way ANOVA, followed by the Dunnet post-test for (* $p<0.05$; ** $p<0.01$; *** $p<0.001$). 93
- Figure 4.3 (A)The cytotoxicity of HepG2 cells lines treated with different concentrations of camptothecin, while untreated HepG2 cells as control. (B) The line graph showed the IC₅₀ of camptothecin treated HepG2 cells. Data are presented as mean±SD, n=3. Comparisons between treatment and untreated were done using one-way ANOVA, followed by the Dunnet post-test for (* $p<0.05$; ** $p<0.01$; *** $p<0.001$)..... 95
- Figure 4.4 (A)The cytotoxicity of THLE-3 cells lines treated with different concentrations of *C. roseus*-AgNPs, while untreated THLE-3 cells and AgNO₃ treatment represent negative control (B) The line graph showed the IC₅₀ of THLE-3 cells treated with *C. roseus*-AgNPs. Data are presented as mean±SD, n=3. Comparisons between treatment and untreated were done using one-way ANOVA, followed by the Dunnet post-test for (* $p<0.05$; ** $p<0.01$; *** $p<0.001$)..... 97
- Figure 4.5 (A) The cytotoxicity of THLE-3 cells lines treated with different concentrations of *C. roseus* aqueous extract, while untreated

	THLE-3 cells and AgNO ₃ treatment represents negative control.	
	(B) The line graph showed the IC ₅₀ of THLE-3 cells treated with <i>C. roseus</i> aqueous extract. Data are presented as mean±SD, n=3. Comparisons between treatment and untreated were done using one-way ANOVA, followed by the Dunnet post-test for (* $p<0.05$; ** $p<0.01$; *** $p<0.001$).....	99
Figure 4.6	(A)The cytotoxicity of THLE-3 cells lines treated with different concentrations of camptothecin, while untreated THLE-3 cells as control. (B) The line graph showed the IC ₅₀ of THLE-3 cells treated with camptothecin. All experiments were done in triplicate, and the data represent means and standard deviation. Data are presented as mean±SD, n=3. Comparisons between treatment and untreated were done using one-way ANOVA, followed by the Dunnet post-test for (* $p<0.05$; ** $p<0.01$; *** $p<0.001$).....	101
Figure 4.7	Morphological assessment of (A) Untreated HepG2 (B) <i>C. roseus</i> -AgNPs treated HepG2 cells (C) camptothecin treated HepG2 cells (D) <i>C. roseus</i> aqueous extract treated HepG2 cells using the IncuCyte ZOOM® system at 10× magnification at 24 hours incubation.....	107
Figure 4.8	Morphological assessment of (A) Untreated HepG2 (B) <i>C. roseus</i> -AgNPs treated HepG2 cells (C) camptothecin treated HepG2 cells (D) <i>C. roseus</i> aqueous extract treated HepG2 cells using the IncuCyte ZOOM® system at 10× magnification at 48 hours incubation.....	108
Figure 4.9	Morphological assessment of (A) Untreated HepG2 (B) <i>C. roseus</i> -AgNPs treated HepG2 cells (C) camptothecin treated HepG2 cells (D) <i>C. roseus</i> aqueous extract treated HepG2 cells using the IncuCyte ZOOM® system at 10× magnification at 70 hours incubation.....	109

Figure 4.10	Morphological assessment of (A) Untreated THLE-3 (B) <i>C. roseus</i> -AgNPs treated THLE-3 cells (C) camptothecin treated THLE-3 cells (D) <i>C. roseus</i> aqueous extract treated THLE-3 cells using the IncuCyte ZOOM® system at 10× magnification at 24 hours incubation.....	111
Figure 4.11	Morphological assessment of (A) Untreated THLE-3 (B) <i>C. roseus</i> -AgNPs treated THLE-3 cells (C) camptothecin treated THLE-3 cells (D) <i>C. roseus</i> aqueous extract treated THLE-3 cells using the IncuCyte ZOOM® system at 10× magnification at 48 hours incubation.....	112
Figure 4.12	Morphological assessment of (A) Untreated THLE-3 (B) <i>C. roseus</i> -AgNPs treated THLE-3 cells (C) camptothecin treated THLE-3 cells (D) <i>C. roseus</i> aqueous extract treated THLE-3 cells using the IncuCyte ZOOM® system at 10× magnification at 70 hours incubation	113
Figure 4.13	The nitrite production of HepG2 cells line of different treatments at (A) 24 hours, (B) 48 hours, and (C) 72 hours. Data are presented as means±SD, n=3. Comparisons of the group were done using one-way ANOVA, followed by Dunnett’s post-test to detect any significant differences between the treated and untreated cells (* $p<0.05$; ** $p<0.01$; *** $p<0.001$). Bonferroni post-test for multiple comparisons to detect any significant differences (+ $p<0.05$; ++ $p<0.01$; +++ $p<0.001$; ns not significant).	115
Figure 4.14	The reactive oxygen species production of HepG2 cells line with different treatments. Camptothecin was used as a positive control, while untreated HepG2 cells were used as a negative control. Data are presented as means±SD, n=3. Comparisons of the group were done using two-way ANOVA, followed by Dunnett’s post-test to detect any significant differences between the treated and untreated cells (* $p<0.05$; ** $p<0.01$; *** $p<0.001$). Bonferroni post-test for multiple comparisons to detect any significant differences (+ $p < 0.05$; ++ $p < 0.01$; +++ $p < 0.001$; ns not significant).	117

Figure 4.15 (A) The intracellular Ca²⁺ production of HepG2 cells line with different treatments at 24 hours. Camptothecin was used as a positive control, while untreated HepG2 cells were used as a negative control. Data are presented as means±SD, n=3. Comparisons of the group were done using two-way ANOVA, followed by Dunnett's post-test to detect any significant differences between the treated and untreated cells (* p<0.05; ** p<0.01; *** p<0.001). Bonferroni post-test for multiple comparisons to detect any significant differences (+ p < 0.05; ++ p < 0.01; +++ p < 0.001; ns not significant). (B) The Intensity (count/second) graph for Ca²⁺ quantification in HepG2 cells for 24 hours, (I) Untreated (II) camptothecin (III) *C. roseus*-AgNPs (IV) *C. roseus* aqueous extract (V)AgNO₃. 119

Figure 4.16 (A) The intracellular Ca²⁺ production of HepG2 cells line with different treatments at 48 hours. Camptothecin was used as a positive control, while untreated HepG2 cells were used as a negative control. Data are presented as means±SD, n=3. Comparisons of the group were done using one-way ANOVA, followed by Dunnett's post-test to detect any significant differences between the treated and untreated cells (* p<0.05; ** p<0.01; *** p<0.001) Bonferroni post-test for multiple comparisons to detect any significant differences (+ p < 0.05; ++ p < 0.01; +++ p < 0.001; ns not significant). (B) The Intensity (count/second) graph for Ca²⁺ quantification in HepG2 cells for 48 hours, (I) Untreated (II) camptothecin (III) *C. roseus*-AgNPs (IV) *C. roseus* aqueous extract (V)AgNO₃..... 120

Figure 4.17 (A) The intracellular Ca²⁺ production of HepG2 cells line with different treatments at 72 hours. Camptothecin was used as a positive control, while untreated HepG2 cells were used as a negative control. Data are presented as means±SD, n=3. Comparisons of the group were done using one-way ANOVA, followed by Dunnett's post-test to detect any significant differences between the treated and untreated cells (* p<0.05; ** p<0.01; *** p<0.001) Bonferroni

post-test for multiple comparisons to detect any significant differences (+ $p < 0.05$; ++ $p < 0.01$; +++ $p < 0.001$; ns not significant). **(B)** The Intensity (count/second) graph for Ca^{2+} quantification in HepG2 cells for 72 hours, **(I)** Untreated **(II)** camptothecin **(III)** *C. roseus*-AgNPs **(IV)** *C. roseus* aqueous extract **(V)**AgNO₃. 121

Figure 4.18 The percentage of JC-1 aggregate polarised state and depolarised state after **(A)** 24 hours, **(B)** 48 hours, and **(C)** 72 hours of HepG2 cells line treated with different treatments. Camptothecin was used as a positive control, while untreated HepG2 cells as a negative control. Data are presented as means±SD, n=3. Comparisons of the group were done using two-way ANOVA, followed by Dunnett’s post-test to detect any significant differences between the treated and untreated cells (* $p < 0.05$; ** $p < 0.01$; *** $p < 0.001$). Bonferroni post-test for multiple comparisons to detect any significant differences (+ $p < 0.05$; ++ $p < 0.01$; +++ $p < 0.001$; ns not significant)..... 123

Figure 4.19 Fluorescence microscopic image of HepG2 cells after staining with JC-1 at 72 hours, 10× magnification. **(A)**Untreated cells; **(B)** *C. roseus* aqueous extract treated cells;**(C)** *C. roseus*-AgNPs treated cells and **(D)** Camptothecin treated cells. FITC (diffuse green J-monomers)=unhealthy cells; Texas Red (punctate red mitochondrial J-aggregates) = healthy cells..... 125

Figure 4.23 The percentage of stained in HepG2 cells after treated with different treatments for 12, 24, 48 and 72 hours Annexin-V/FITC/PI analysis by flow cytometry. Data are presented as means±SD, n=3. Comparisons of the group were done by using 2-way ANOVA, followed by the Bonferroni post-test for multiple comparisons. Significant different of treatments compared to untreated cells marked as * $p < 0.05$; ** $p < 0.01$; *** $p < 0.001$ whereas significant different between treatments represent as + $p < 0.05$; ++ $p < 0.01$; +++ $p < 0.001$ 134

- Figure 4.24 DNA histogram of HepG2 cells treated with (A) untreated, (B) camptothecin, (C) *C. roseus*-AgNPs, (D) *C. roseus* aqueous extract and (E) AgNO₃ at 24 hours exposure time. The bar graph shows the quantitative data are based on DNA histograms. Data are presented as means±SD, n=3. Comparisons of the group were done using one-way ANOVA, followed by Dunnett's post-test to detect any significant differences between the treated and untreated cells (* $p < 0.05$; ** $p < 0.01$; *** $p < 0.001$)..... 138
- Figure 4.25 DNA histogram of HepG2 cells treated with (A) untreated, (B) camptothecin, (C) *C. roseus*-AgNPs, (D) *C. roseus* aqueous extract and (E) AgNO₃ at 48 hours exposure time. The bar graph shows the quantitative data are based on DNA histograms. Data are presented as means±SD, n=3. Comparisons of the group were done using one-way ANOVA, followed by Dunnett's post-test to detect any significant differences between the treated and untreated cells (* $p < 0.05$; ** $p < 0.01$; *** $p < 0.001$). 139
- Figure 4.26 DNA histogram of HepG2 cells treated with (A) untreated, (B) camptothecin, (C) *C. roseus*-AgNPs, (D) *C. roseus* aqueous extract, and (E) AgNO₃ at 72 hours exposure time. The bar graph shows the quantitative data are based on DNA histograms. Data are presented as means±SD, n=3. Comparisons of the group were done using one-way ANOVA, followed by Dunnett's post-test to detect any significant differences between the treated and untreated cells (* $p < 0.05$; ** $p < 0.01$; *** $p < 0.001$)..... 140
- Figure 4.27 Tail DNA percentage of HepG2 cells lines treated with different treatments at (A) 24 hours, (B) 48 hours, and (C) 72 hours. Data are presented as means±SD, n=3. Comparisons of the group were done using one-way ANOVA, followed by Dunnett's post-test to detect any significant differences between the treated and untreated cells (* $p < 0.05$; ** $p < 0.01$; *** $p < 0.001$). Bonferroni post-test for multiple comparisons to detect any significant differences (+ $p < 0.05$; ++ $p < 0.01$; +++ $p < 0.001$; ns not significant). 142

- Figure 4.28 (A) The intracellular Ag uptake of HepG2 cells line at 24, 48, and 72 hours. Data are presented as means±SD, n=3. Comparisons of the group were done using two-way ANOVA, followed by Dunnett's post-test to detect any significant differences between the treated and untreated cells (* $p < 0.05$; ** $p < 0.01$; *** $p < 0.001$). Bonferroni post-test for multiple comparisons to detect any significant differences (+ $p < 0.05$; ++ $p < 0.01$; +++ $p < 0.001$; ns not significant). (B) The Intensity (count/second) graph for Ag quantification in HepG2 cells, *C. roseus*-AgNPs (I) 24hours (II) 48hours (III)72 hours; AgNO₃ (IV) 24 hours (V)48 hours (VI)72hours. 145
- Figure 4.29 (A) The exocytosis of Ag from HepG2 cells line at 24, 48, and 72 hours. Data are presented as means±SD, n=3. Comparisons of the group were done using two-way ANOVA, followed by Dunnett's post-test to detect any significant differences between the treated and untreated cells (* $p < 0.05$; ** $p < 0.01$; *** $p < 0.001$). Bonferroni post-test for multiple comparisons to detect any significant differences (+ $p < 0.05$; ++ $p < 0.01$; +++ $p < 0.001$; ns not significant). (B) The Intensity (count/second) graph of Ag from HepG2 cells, *C. roseus*-AgNPs (I) 24hours (II) 48hours (III)72 hours; AgNO₃ (IV) 24 hours (V) 48 hours (VI)72hours..... 147
- Figure 4.30 Comparison of exocytosis and endocytosis of Ag in HepG2 cells treated with *C. roseus*-AgNPs. All experiments were done in triplicate, and the data represent means ± standard deviation. Comparison between exocytosis, endocytosis was done using two-way ANOVA with Bonferroni post-test for multiple comparisons to detect any significant differences (* $p < 0.05$; ** $p < 0.01$; *** $p < 0.001$; ns not significant)..... 149
- Figure 4.31 (A) The endocytosis of *C. roseus*-AgNPs was studied in response to selective inhibitors using HepG2 cells for 24 hours. Data are presented as means±SD, n=3. Comparisons of the group were done using two-way ANOVA, followed by Dunnett's post-test to detect any significant differences between the treated and untreated cells

(* $p < 0.05$; ** $p < 0.01$; *** $p < 0.001$). Bonferroni post-test for multiple comparisons to detect any significant differences (+ $p < 0.05$; ++ $p < 0.01$; +++ $p < 0.001$; ns not significant). **(B)** The Intensity (count/second) graph of Ag from HepG2 cells, *C. roseus*-AgNPs **(I)** without inhibitor **(II)** K^+ depletion media **(III)** Wortmannin **(IV)** Nystatin. 152

Figure 4.32 **(A)** The endocytosis of *C. roseus*-AgNPs was studied in response to selective inhibitors using HepG2 cells for 48 hours. Data are presented as means \pm SD, n=3. Comparisons of the group were done using two-way ANOVA, followed by Dunnett's post-test to detect any significant differences between the treated and untreated cells (* $p < 0.05$; ** $p < 0.01$; *** $p < 0.001$). Bonferroni post-test for multiple comparisons to detect any significant differences (+ $p < 0.05$; ++ $p < 0.01$; +++ $p < 0.001$; ns not significant). **(B)** The Intensity (count/second) graph of Ag from HepG2 cells, *C. roseus*-AgNPs **(I)** without inhibitor **(II)** K^+ depletion media **(III)** Wortmannin **(IV)** Nystatin. 153

Figure 4.33 **(A)** The endocytosis of *C. roseus*-AgNPs was studied in response to selective inhibitors using HepG2 cells for 72 hours. Data are presented as means \pm SD, n=3. Comparisons of the group were done using two-way ANOVA, followed by Dunnett's post-test to detect any significant differences between the treated and untreated cells (* $p < 0.05$; ** $p < 0.01$; *** $p < 0.001$). Bonferroni post-test for multiple comparisons to detect any significant differences (+ $p < 0.05$; ++ $p < 0.01$; +++ $p < 0.001$; ns not significant). **(B)** The Intensity (count/second) graph of Ag from HepG2 cells, *C. roseus*-AgNPs **(I)** without inhibitor **(II)** K^+ depletion media **(III)** Wortmannin **(IV)** Nystatin. 154

Figure 4.34 Electron micrographs of HepG2 treated with *C. roseus*-AgNPs at 24 hours. **(A)** Untreated HepG2 cells **(B)** Intracellular accumulation of *C. roseus*-AgNPs in HepG2 cells. **(I)** Formation of plasma membrane protrusion (black arrow). **(II)** Cell shows *C. roseus*-AgNPs in the cytosol. 156

Figure 4.35	Electron micrographs of HepG2 treated with <i>C. roseus</i> -AgNPs at 48 hours. (A) Untreated HepG2 cells (B) Intracellular accumulation of <i>C. roseus</i> -AgNPs in HepG2 cells. (I) Plasma membrane protrusion fold back forming caved-like invagination (black arrow) and (yellow arrow) showed <i>C. roseus</i> -AgNPs near membrane. (II) Cell shows <i>C. roseus</i> -AgNPs in the cytosol.	157
Figure 4.36	Electron Micrographs of HepG2 treated with <i>C. roseus</i> -AgNPs at 72 hours. (A) Untreated HepG2 cells (B) <i>C. roseus</i> -AgNPs deposited in HepG2 cells. (I) <i>C. roseus</i> -AgNPs in endosomes/lysosome (black arrow), <i>C. roseus</i> -AgNPs being exocytosed (yellow arrow) (II) <i>C. roseus</i> -AgNPs in the exocytic vesicles (black arrow), <i>C. roseus</i> -AgNPs being exocytosed (yellow arrow).....	158
Figure 4.37	Representative electropherograms by bioanalyser (a) The RNA samples for untreated HepG2 cells (b) the RNA samples for <i>C. roseus</i> -AgNPs treated HepG2 cells.	160
Figure 4.38	Filter composition of raw data. a) RNA samples for untreated HepG2 cells (b) RNA samples for <i>C. roseus</i> -AgNPs treated HepG2 cells. N: The total amount of reads which contain more than 5% unknown N base; Adaptor: The total amount of reads which contain adaptors; Low quality: More than 20% of bases in the total read have a quality score lower than 15; Clean reads: Reads filtered with N reads, reads have adaptors, and low-quality reads.	162
Figure 4.39	Distribution of base quality on clean reads. X axis represents base positions along reads. The Y axis represents base quality value. Each dot in the image represents the number of total bases with certain quality value of the corresponding base along reads. a) untreated HepG2, b) <i>C. roseus</i> -treated HepG2.	164
Figure 4.40	Distribution of SNP location a) Untreated HepG2 b) <i>C. roseus</i> -AgNPs treated HepG2. Up2k means upstream 2,000 bp area of a gene. Down2k means downstream 2,000 bp area of a gene.	167
Figure 4.42	Statistic of splicing	170

Figure 4.45	Heatmaps of DEGs for <i>C. roseus</i> -AgNPs treated cells. Each row represents a gene. Red and blue represent high and low expression levels, respectively.....	184
Figure 4.46	KEGG-DEG (differential expression gene) relationship network. The green colour represents the downregulated genes. The red colour represents the upregulated genes. The brighter the colour indicates the higher the log fold change.....	187
Figure 5.1	The proposed oxidative stress and mitochondrial depolarisation induced by <i>C. roseus</i> -AgNPs based on the experimental data obtained in the present study. Created with BioRender.com.....	200
Figure 5.2	Schematic diagram showing the potential mechanism underlying apoptosis induction in HepG2 cells treated with <i>C. roseus</i> -AgNPs	206
Figure 5.2	Schematic diagram showing the possible endocytosis and exocytosis patterns of <i>C. roseus</i> -AgNPs which involved macropinocytosis and clathrin mediated endocytosis. Exocytosis of <i>C. roseus</i> -AgNPs involved lysosome secretion and non-vesical secretion. Created with BioRender.com	213
Figure 5.3	Schematic diagram of cell death mechanism induced by <i>C. roseus</i> -AgNPs in HepG2 cells. The <i>C. roseus</i> -AgNPs treatment triggered apoptosis in HepG2 cells two major pathways: the cell-death-receptor-mediated (extrinsic) apoptotic pathway and the mitochondrial-mediated (intrinsic) apoptotic pathway which involved the underlying pathways regulated by the genes which were p53 signalling pathway, apoptosis pathway, endocytic pathway, MAPK signalling pathway, TNF signalling pathway, TGF signalling pathway, and cell cycle pathway.....	216

LIST OF ABBREVIATIONS

AgNPs	Silver nanoparticles
Ag ⁺	Silver ion
Ag ⁰	Silver
Ar	Argon
3D	Three-dimensional
ANOVA	Analysis of variance
ATCC	American Tissue Culture Collection
BEGM	Bronchial Epithelial Cell Growth Basal Medium
C	Carbon
Ca	Calcium
Ca ²⁺	Calcium ion
CaO	Calcium oxide
CDK	Cyclin-dependent kinase
CDKI	CDK inhibitor
cDNA	Complementary DNA
CO ₂	Carbon dioxide
DC	Direct current
DCFH-DA	2, 7-dichlorodihydrofluorescein diacetate
DCM	Dichloromethane
DD	Death domain
DDIT3	DNA damage-inducible transcript
DEG	Differentially expressed genes
DISC	Death-inducing signalling complex
DMEM	Dulbecco's Modified Eagle Medium,
DMSO	Dimethyl sulfoxide

DNA	Deoxyribonucleic acid
DNBs	DNA nanoballs
DTT	Dithiothreitol
DUSP	Dual-specificity phosphatase
EDTA	Ethylenediaminetetraacetic acid
EMA	European Medicines Agency
EGF	Epidermal growth factor
ER	Endoplasmic reticulum
ERK	Extracellular signal-regulated kinase
EST	Expressed sequence tag
FBS	Fetal bovine serum
FDA	U.S. Food and drug administration
FITC	Fluorescein isothiocyanate
FPKM	Fragments per kilobase million
FTIR	Fourier transform infrared spectroscopy
G0	Gap G0 growth phase
G0/G1	Checkpoint occurs between the G0 and G1 phases
G1	Gap G1 growth phase
G2	Gap G2 growth phase
G2/M	Checkpoint occurs between the G2 and M phases
GLOBOCAN	Global Cancer Observatory
GO	Gene ontology
GPI	Glycosylphosphatidylinositol
GTN	Goniothalamine
GTN-BG	Combination of GTN and BG
H	Hydrogen
H ₂ O	Water

HCC	Hepatocellular carcinoma
HEPG2	Hepatocellular carcinoma cell line
HIV	Human immunodeficiency viruses
HNO ₃	Nitric acid
HPV	Human papillomavirus
IC ₅₀	Half maximal inhibitory concentration
ICP-OES	Inductively coupled plasma optical emission spectrometry
IR	Infrared
JNK	C-Jun N-terminal kinase
JC-1	Cationic carbocyanine dye
K	Potassium
K ⁺	Potassium ion
KBr	Potassium bromide
LED	Light-emitting diode
LDL	Low-density lipoprotein
M	Mitotic phase
MAPK	Mitogen-activated protein kinase
MCF-7	Human breast adenocarcinoma cells
Mg	Magnesium
Mg ²⁺	Magnesium ion
mRNA	messenger ribonucleic acid
MTT	3-(4,5-dimethylthiazol-2-yl)-2,5-diphenyltetrazolium bromide
Na	Sodium
Na ⁺	Sodium ion
NADH	Nicotinamide adenine dinucleotide hydrogen
NP	Nanoparticles

NGS	Next-generation sequencing
NO	Nitric oxide
n	Sample size
ns	Not significant
NSPCCP	National Strategic Plan for Cancer Control Programme
O	Oxygen
OD	Optical density
OH	Hydroxyl group
P	Phosphorus
PBS	Phosphate-buffered saline
PCR	Polymerase chain reaction
PEG	Polyethylene glycol
PI	Propidium iodide
PLK5	Polo-like kinase 5
PO ₄ ³⁻	Phosphate ion
PSI	Pounds per square inch
PVP	Polyvinylpyrrolidone
QC	Quality control
RIN	RNA integrity number
RNA	Ribonucleic acid
ROS	Reactive oxygen species
RPM	Revolution per minute
RPMI 1640	Roswell Park Memorial Institute 1640
S	Synthesis phase
SAED	Selected-area electron diffraction
SD	Standard deviation
SDS	Sodium dodecyl sulphate

SEM	Standard error of the mean
SEM-EDS	Scanning electron microscopy-elemental analysis
SI	Selectivity index
Si	Silicon
SiO ₂	Silicon dioxide
Si-OH	Silanol group
TEM	Transmission electron microscopes
THLE-3	Normal liver cell line
SI	Tumour selective index
TGF-β	Transforming growth factor-β
TNFRSF	Tumour necrosis factor receptor superfamily
TIAs	Terpenoid indole alkaloids
UACC	Human breast carcinoma cells
USA	United States of America
UT	Untreated sample
UV	Ultraviolet
UV VIS	Ultraviolet-Visible spectroscopy
WHO	World Health Organization
XRD	X-ray diffraction

LIST OF UNITS

°C	Degree celcius
μg	Microgram
μL	Microliter
μm	Micrometer
μM	Micromolar
Å	Ångström
cells/mL	Cells per millilitre
cm ⁻¹	Reciprocal wavelength
cm ²	Centimeter square
cm ³ /g	Centimeter cubic per gram
c/s	Count/second
Da	Dalton
g	Gram (weight per unit mass)
<i>g</i>	Gravity
Hz	Hertz
kV	Kilovolt
M	Molar
m ² /g	Meter square per gram
mA	Milliampere
mg/mL	Milligram per mililiter
MHz	Megahertz
min	Minute
mL	Milliliter
mm	Millimeter
mM	Millimolar

mV	Millivolt
nm	Nanometer
nM	Nanomolar
PPM	Parts per million
psi	Pounds per square inch
RFU	Relative fluorescence units
U/mL	Units per milliliter
v/v	Volume/volume
w/v	Weight/volume

LIST OF SYMBOLS

α	Alpha
β	Beta
δ	Delta
θ	Theta
\sim	Approximately
*	Asterisk
–	Dash
=	Equals
>	Greater than
-	Hyphen
<	Less than
\leq	Less-than or equal to
/	Or
\pm	Plus-minus
®	Registered trademark
×	Times
™	Trademark
%	Percentage
+	Plus
$\Delta\psi_m$	Mitochondria membrane potential

LIST OF APPENDICES

- Appendix A Calculation of 5mM AgNO₃
- Appendix B The standard curve of nitrite concentration
- Appendix C Library Construction

**KAJIAN KE ATAS KESAN *Catharanthus roseus*- NANOPARTIKEL PERAK
TERHADAP SEL SELANJAR KARSINOMA HEPATOSELULAR MANUSIA
HEPG2**

ABSTRAK

Kanser merupakan cabaran kesihatan global yang signifikan dan terus meningkat di seluruh dunia serta menjadi penghalang utama untuk mencapai jangka hayat yang panjang. Ubat-ubatan kemoterapi konvensional yang bersifat kurang selektif, menimbulkan kesan sampingan yang besar serta membahayakan sel sihat. Oleh itu, terapi kanser alternatif adalah penting, dan penggunaan nanopartikel perak (AgNPs) membentuk pendekatan baru dalam rawatan kanser disebabkan ciri uniknya. Penggunaan tumbuhan untuk biosintesis AgNPs menawarkan beberapa kelebihan berbanding dengan kaedah lain. Beberapa kajian telah melaporkan bahawa sintesis AgNPs melalui tumbuhan mempunyai aktiviti antikanser terhadap pelbagai jenis sel kanser. Oleh itu, kesan antiproliferasi dan indeks pemilihan (SI) nanopartikel perak *Catharanthus roseus* (*C. roseus*-AgNPs) terhadap sel sasaran hepatoselular karsinoma (HepG2) ditentukan dengan menggunakan sel hati bukan sasaran manusia (THLE-3) sebagai kawalan. *C. roseus*-AgNPs menunjukkan kesan antiproliferasi yang lebih poten daripada ekstrak akueus *C. roseus* dalam menghalang proliferasi sel HepG2 sementara menunjukkan kesan antiproliferasi yang lebih rendah terhadap sel THLE-3. *C. roseus*-AgNPs menunjukkan kesan ketoksikan yang selektif terhadap sel HepG2 dengan nilai SI yang tinggi (>2) berbanding dengan camptothecin. Bagi kedua-dua rawatan *C. roseus*-AgNPs dan ekstrak akueus *C. roseus*, beberapa ciri apoptotik telah dikesan apabila diperhatikan menggunakan sistem analisis sel hidup IncuCyte, termasuk pengecutan sel.

Mekanisme yang terlibat dengan kesan perencatan pada sel yang dirawat telah dikaji secara lebih mendalam. Peningkatan tahap ROS, NO dan Ca^{2+} , bersama-sama dengan kehilangan MMP dianggap sebagai pencetus tekanan oksidatif. Kajian ini juga menunjukkan bahawa apoptosis diaktifkan melalui laluan kematian ekstrinsik dan laluan mitokondria intrinsik, kerana pengaktifan kaspase eksekutor dan efektor dikesan dalam sel HepG2 yang dirawat dengan *C. roseus*-AgNPs. Memandangkan pengaktifan kaspase telah dikaitkan dengan pemutusan rantai DNA dan penahanan kitaran sel, potensi genotoksik *C. roseus*-AgNPs telah dikaji dengan lebih lanjut. Dapatan menunjukkan bahawa sel HepG2 yang dirawat dengan *C. roseus*-AgNPs menunjukkan kerosakan DNA yang ketara dan penahanan serentak dalam progresi kitaran sel pada G₂/M. Persepsi yang lebih mendalam boleh dicapai melalui pemahaman dengan lebih mendalam tentang mekanisme pengambilan selular mereka. Oleh itu, pengambilan selular *C. roseus*-AgNPs telah dikaji lebih lanjut dengan melihat pengumpulan Ag intrasel dan seterusnya menilai taburan *C. roseus*-AgNPs dalam sel HepG2. Sel HepG2 utamanya mengambil *C. roseus*-AgNPs melalui endositosis bergantung kepada klatrin dan makropinoktosis, seperti yang dibuktikan dengan peningkatan gen yang terlibat dalam endositosis, pembentukan protrusi membran plasma, dan penghalangan klatrin melalui medium terdepleksi K⁺. Bagi memahami mekanisme aktiviti antikanser *C. roseus*-AgNPs terhadap sel HepG2, adalah perlu untuk mengenal pasti gen yang bekerjasama untuk menghasilkan kesan tersebut. Analisis transkriptomik, yang memberikan pandangan menyeluruh tentang ekspresi gen dalam keadaan tertentu, digunakan untuk menyiasat profil ekspresi gen dan memperoleh pemahaman mendalam tentang sifat antikanser *C. roseus*-AgNPs. Kajian ini menunjukkan bahawa rawatan dengan *C. roseus*-AgNPs menyebabkan peningkatan ekspresi gen tindakbalas Tumour dan apoptosis dalam sel HepG2, serta

pengaktifan beberapa laluan pemindahan isyarat termasuk laluan MAPK, endositosis, TNF, dan laluan TGF-Beta serta penahanan kitaran sel. Kesimpulannya, *C. roseus*-AgNPs mempunyai aktiviti antikanser yang kuat dan selektif terhadap sel HepG2 melalui mekanisme yang melibatkan tekanan oksidatif, apoptosis, kerosakan DNA, dan penahanan kitaran sel. Pemahaman yang diperolehi menunjukkan bahawa *C. roseus*-AgNPs boleh menjadi alternatif atau pelengkap yang baik kepada kemoterapi konvensional, menawarkan rawatan kanser yang disasarkan dengan potensi kesan sampingan yang kurang.

**STUDY ON THE EFFECTS OF *Catharanthus roseus*-SILVER
NANOPARTICLES ON HUMAN HEPATOCELLULAR CARCINOMA
CELL LINE HEPG2**

ABSTRACT

Cancer is a major global health challenge that continues to increase worldwide, posing a significant obstacle to achieving long life expectancy. Conventional chemotherapy drugs may not be specific enough, leading to significant side effects and harm to healthy cells. Therefore, alternative cancer therapies are crucial, and application of silver nanoparticles (AgNPs) presents a novel approach to cancer treatment due to their unique features. Utilising plants for the biosynthesis of AgNPs offers several advantages over other methods. Numerous studies had reported that plant mediated AgNPs synthesis have been found to exhibit potent anticancer activity against various cancer cell lines. Thus, the antiproliferative effects and selective index (SI) of *Catharanthus roseus*-silver nanoparticles (*C. roseus*-AgNPs) on hepatocellular carcinoma (HepG2) cells were determined by using normal liver cell line (THLE-3) as a control. *C. roseus*-AgNPs was more potent than *C. roseus*-aqueous extract in inhibiting the proliferation of HepG2 cells while exhibiting less inhibition towards THLE-3 cells. *C. roseus*-AgNPs demonstrated selective toxicity towards HepG2 cells with a high SI value (>2) compared to camptothecin. For both *C. roseus*-AgNPs and *C. roseus*-aqueous extract treatments, several apoptotic features were detected when observed using IncuCyte live-cell analysis system, including cell shrinkage, rounded cells, and retracted. The underlying mechanisms associated with the inhibitory effects in the treated cells were further explored. The increased level of ROS, NO and Ca²⁺ levels, together with the subsequent loss of MMP was assumed to induced oxidative

stress. This study also depicted that apoptosis was triggered through both extrinsic death receptor pathway and intrinsic mitochondrial pathway as the activation of executioner and effector caspases were detected in *C. roseus*-AgNPs treated HepG2 cells. Given that caspase activation has been implicated in DNA strand breaks and cell cycle arrest, the genotoxic potential of *C. roseus*-AgNPs was further assessed. The findings indicate that HepG2 cells treated with *C. roseus*-AgNPs exhibit significant DNA damage and concurrent arrest of cell cycle progression at G₂/M. In-depth perception of the cytotoxic effects of *C. roseus*-AgNPs on HepG2 cells can be achieved through a better understanding of their cellular uptake mechanisms. Therefore, the *C. roseus*-AgNPs cellular uptake was further explored by looking at the accumulation of intracellular Ag followed by the evaluation of the *C. roseus*-AgNPs distribution in HepG2 cells. HepG2 cells primarily took up *C. roseus*-AgNPs through clathrin-dependent endocytosis and macropinocytosis, as evidenced by upregulated genes involved in endocytosis, the formation of plasma membrane protrusions, and the inhibition of clathrin through K⁺ depleted medium. To comprehend the underlying mechanisms of the anti-cancer activity of *C. roseus*-AgNPs against HepG2 cells, it is necessary to identify the genes that collaborate to produce the effect. Transcriptome analysis, which provides a comprehensive view of gene expression under a specific condition, was used to investigate the gene expression profile, and gain an in-depth understanding of the anti-cancer properties of *C. roseus*-AgNPs. The study found that treatment with *C. roseus*-AgNPs led to increased expression of tumour suppressor and apoptotic genes in HepG2 cells, as well as activation of several signal transduction pathways including the MAPK, endocytosis, TNF, and TGF-Beta pathways as well as cell cycle arrest. In conclusion, *C. roseus*-AgNPs exhibit potent and selective anticancer activity against HepG2 cells through mechanisms involving oxidative

stress, apoptosis, DNA damage, and cell cycle arrest. The molecular insights gained indicate that *C. roseus*-AgNPs could be a promising alternative or complement to conventional chemotherapy, offering targeted cancer treatment with potentially fewer side effects.

CHAPTER 1

INTRODUCTION

1.1 Background

Cancer is a complex and multifaceted disease that affects millions of people worldwide. According to the World Health Organization (WHO), cancer was the leading cause of death globally in 2020, accounting for nearly 10 million deaths in 2022. The most common cancer with high mortality rate in 2020 were lung, colon, liver, stomach, and breast cancers. Hepatocellular carcinoma (HCC), also known as liver cancer, is a type of cancer that originates in the liver cells, called hepatocytes. It is the most common type of liver cancer, accounting for more than 700,000 deaths each year (Siegel *et al.*, 2023). In Malaysia, liver cancer is one of the ten most frequent cancers diagnosed in patients (Mohamed *et al.*, 2018). While other types of liver cancer, such as cholangiocarcinoma and hepatoblastoma, are also important, HCC's higher prevalence and impact on public health make it a primary focus of research in liver cancer (Reghupaty *et al.*, 2021).

There are several types of conventional treatments for liver cancer including surgery, chemotherapy, radiation therapy and immunotherapy, that can cause significant side effects and toxicity. These treatments not only affect cancer cells but can also harm the healthy cells and tissues, leading to adverse effects such as fatigue, nausea, hair loss, and reduced immune function. These side effects can impact the patient's quality of life and limit the treatment tolerability (Andleeb *et al.*, 2021). Other types of cancer treatments include targeted therapy, hormone therapy, and stem cell transplant. The type of treatment chosen will be determined by various criteria, including the type of cancer, its stage, and the patient's overall condition (Sanità *et al.*, 2020). Due to the limitation of conventional treatments for liver cancer, thus, the

search for a novel approach and discover potent anticancer agents for effective treatment against cancer with minimal side effects becomes prominent. Nanotechnology-based approaches have shown promising potential such as maximal efficacy and safety to ameliorate cancer therapy and diagnosis in recent years (Shabani *et al.*, 2022). Nanoparticles possess unique characteristics such as nanosized particle which are large surface area per volume ratio, porosity, solubility, bioavailability and have various structural properties. Due to the unique characteristics of the nanoparticle, a nanoscale anticancer drug has developed into a high-benefit treatment since it has high stability and specificity, is durable and less dosed frequency needed (Sinha *et al.*, 2006).

Silver nanoparticles (AgNPs) enticed the attention of the scientific community and trade itself by exploiting several biomedical applications including diagnosis, treatment, medical device coatings, drug delivery, personal health care product, antimicrobial agents, anti-inflammatory agents, and anticancer agents. AgNPs can be synthesized through various methods including the physical, chemical, biological and hybrid methods (Iravani *et al.*, 2014). Among preparation techniques that have been reported for the synthesis of AgNPs including laser ablation, gamma and electron irradiation, chemical reduction method, microemulsion technique, UV-initiated photoreduction methods, electrochemical synthetic method, microwave-assisted synthesis, Tollen method and biological synthetic methods (Abbasi *et al.*, 2013.; Gurunathan *et al.*, 2013; Kaviya *et al.*, 2014). There are potentials and limitations of physical and chemical methods although these techniques serve as an imperative technique in the synthesis of AgNPs. The main drawback of these methods is that they are extremely high cost, and very toxic to human being since there are involvement of hazardous and high toxicity chemicals such as sodium borohydride, potassium

bitartrate, methoxy polyethylene glycol and hydrazine which function in reducing the sizes of particles (Le *et al.*, 2010; Prabhu *et al.*, 2013; Bagherzade *et al.*, 2017).

Therefore, here is a growing need to develop an eco-friendly and financially doable approach to the technique of synthesising AgNPs. The hunt for such a method has led to the biogenic synthesis of silver nanoparticles which are more eco-friendly, hazard-free, easily accessible, and cost-effective (Kaviya *et al.*, 2014). Therefore, biosynthesis of AgNPs using bacteria, fungi, or plants has been a major approach since this method offers a fascinating alternative to chemical synthesis (Ahmed *et al.*, 2016). AgNPs synthesised by plants are more effective, as in plants, they are effortlessly accessible, safe and nontoxic much of the time and they also have an expansive mixed bag of metabolites that can help in the reduction of silver ions (Piao *et al.*, 2011; Prabhu *et al.*, 2013; Sankar *et al.*, 2013).

Catharanthus roseus (L.) G. Don, also known as the Madagascar periwinkle, is a medicinal plant classified under the Apocynaceae family that synthesises terpenoid indole alkaloids (TIAs) (Moudi *et al.*, 2013). Additionally, *C. roseus* acts as a reducing and stabilising agent in the synthesis of nanoparticles due to its rich content of phytochemicals. This plant contains several active compounds, including vinblastine and vincristine, which are commercially available tubulin inhibitors (TIAs) used in chemotherapy for cancer treatment. These compounds belong to a group of compounds called the vinca alkaloids, which repress cell growth by altering the microtubular dynamics, ultimately provoking apoptosis. They are commonly used to treat several malignant conditions, including Hodgkin's and non-lymphomas, Hodgkin's acute lymphoblastic leukaemia, neuroblastoma, and breast carcinoma (Ghozali *et al.*, 2018).

Based on the facts that inorganic-based NPs have been successfully used clinically and biosynthesis of AgNPs provides more advantages, we envisage possible

anticancer effects of *C. roseus*-AgNPs to rule out the biosafety issues of AgNPs and provide theoretical basis to develop a better anticancer therapeutic strategy for HCC - to rule out the biosafety issues of AgNPs and provide a theoretical basis to develop a better anticancer therapeutic strategy for HCC.

1.2 Rationale of study

Hepatocellular carcinoma (HCC) is one of the most common and deadliest types of liver cancer that arises from the hepatocytes, the main type of liver cells responsible for carrying out essential functions such as detoxification, protein synthesis, and bile production (Llovet *et al.*, 2021). HCC is known for its aggressive nature and resistance to conventional treatments such as chemotherapy and radiation therapy. Surgical resection and liver transplantation are potentially curative treatments for early-stage HCC, but these treatments are not feasible for all patients due to factors such as the presence of underlying liver disease, the size and location of the Tumour, and the patient's overall health. Another limitation of conventional treatments is the potential for toxicity and side effects, including the inability to target specific sites that can lead to long-term health consequences and the potential for cancer recurrence (Huang *et al.*, 2020). Due to the limitations of traditional treatments for HCC, there is a need for the development of novel and effective therapies for this disease. Therefore, researchers are constantly exploring new compounds with strong anticancer activity and minimal toxicity towards untargeted cells as potential alternatives to conventional chemotherapeutic drugs. The development of such compounds is crucial to improve cancer treatment and reducing the side effects associated with current therapies. While previous study exploring the cytotoxic effects of *C. roseus*-AgNPs in cancer cell lines, less attention has been made to their selectivity in human cancer cell lines (Ghozali *et*

al., 2015). It is essential to determine the selectivity of *C. roseus*-AgNPs in cancer cell lines versus normal human cells as this can help assess their safety for use in cancer therapy. Selectivity refers to the ability of a therapeutic agent to target cancer cells while sparing untargeted cells, minimising side effects (Rashidi *et al.*, 2017). Therefore, in this study, the antiproliferative effects of *C. roseus*-AgNPs were evaluated on hepatocellular carcinoma (HepG2) cells and normal liver (THLE-3) cells. THLE-3 cells are a human liver cell line that has been widely used as a normal control cell line in many studies involving liver cancer cells (Jehan *et al.*, 2020). Two vital parameters were measured; the half maximum inhibitory concentration (IC₅₀) to study the efficacy of *C. roseus*-AgNPs in inhibiting cancer cells and the tumour selectivity index (TSI) to examine the safety of *C. roseus*-AgNPs as a therapeutic candidate to untargeted cells.

Silver nanoparticles are a more commonly used in research than gold nanoparticles due to several reasons. Firstly, silver is less expensive than gold, which makes it a more affordable option for researchers who want to study nanoparticles (Devi *et al.*, 2022). AgNPs can be synthesised more easily and in larger quantities than gold nanoparticles, which can be challenging to produce in a consistent and reproducible manner (Solati and Dorrnian, 2015). One justification is related to the surface properties of silver nanoparticles, which can enhance their cellular uptake and cytotoxicity against cancer cells. Studies have shown that AgNPs can accumulate more efficiently in cancer cells compared to untargeted cells, due to their preferential interaction with the tumour microenvironment and cancer cell membranes. This increased uptake can enhance their therapeutic efficacy while reducing their toxicity to untargeted cells (Talarska *et al.*, 2021). In contrast, gold nanoparticles are generally considered to have low cellular uptake and require additional modifications to enhance

their tumour targeting and uptake. This can limit their efficacy in some cancer therapy applications (Huang *et al.*, 2006). Another justification is related to the unique optical properties of gold nanoparticles, which can limit their usefulness in certain applications. Gold nanoparticles have a distinct colour due to their plasmon resonance, which can interfere with some types of imaging techniques and biosensors (Lynch and Dawson, 2008). In contrast, silver nanoparticles have a broader absorption spectrum, which can make them more suitable for some types of imaging and sensing applications (Solati and Dorrnian, 2015). While gold nanoparticles have their own unique advantages, silver nanoparticles are often the preferred choice in much research. Hence, AgNPs were selected to be greenly synthesised in this study.

There are several approaches to synthesising AgNPs such as chemical, physical, and biological approaches. Biological approaches have been shown to be the most economical, sustainable, reliable, and eco-friendly of all AgNPs synthesis approaches, and this approach does not use harmful chemicals (Andleeb *et al.*, 2021). The synthesis of AgNPs using plants offers several benefits, such as biocompatibility, easy and low-cost synthesis, environmentally friendly, and had potential for additional bioactive properties making it a promising approach for the development of safe and effective nanomaterials (Xu *et al.*, 2020). Thus, this study was designed to explore the cytotoxicity of plant mediated synthesis of AgNPs (*C. roseus*-AgNPs) on HepG2 cells.

Defects in cell death pathways, such as apoptosis and autophagy, can contribute to cancer development and progression, which is one of the hallmarks of cancer. Many cancer treatments aim to boost the ability of cancerous cells to undergo programmed cell death, either by activating apoptotic pathways or by inhibiting pro-survival pathways (Thapa *et al.*, 2022). Identifying the mechanisms underlying apoptosis, as well as its effector proteins and genes, can aid in the discovery of novel

anticancer treatments that boost cancer cell sensitivity to apoptosis. Therefore, the underlying mechanisms associated with the inhibitory effects in the *C. roseus*-AgNPs treated cells were further explored in this study. This study provides insight into the underlying molecular mechanisms of cell death, specifically by apoptosis in cells treated with *C. roseus*-AgNPs. It will be useful for further evaluation in preclinical and clinical settings for cancer treatment.

An understanding of the anticancer mechanisms of AgNPs at the molecular level would provide detailed insight into various physiological processes involved. This is achievable via transcriptome analysis, a holistic view of gene expression. An overview or snapshot of the gene expression landscape could reveal the intricate molecular network that underlies the myriad of biological processes in a cell. As compared to hybridisation-based RNA quantification methods such as microarray analysis, this sequencing-based transcriptome detection can perform well within a wide range of circumstances, where this method could quantify gene expression with low background, high accuracy, and high reproducibility levels with significant dynamic range transcriptome analysis can detect subtle changes in gene expression, mutations, splice variants and fusion genes that cannot be identified by microarrays. Fuelled by the intriguing capacity of the transcriptome analysis, in this study, we endeavoured to carry out an mRNA transcriptome profiling of the *C. roseus*-AgNPs treated HepG2 cells.

1.3 Research objectives

This study has five main objectives, and the following specific objectives have been developed to achieve the main goals.

1. To elucidate the antiproliferative effects of *C. roseus*-AgNPs on HepG2 and THLE-3 cells.
 - a. To identify the IC₅₀ values of *C. roseus*-AgNPs, *C. roseus* aqueous extract, and camptothecin on HepG2 and THLE-3 cells.
 - b. To compare the antiproliferative effectiveness of *C. roseus*-AgNPs, *C. roseus* aqueous extract, and camptothecin on HepG2 and THLE-3 cells.
 - c. To calculate the Selectivity Index (SI) of *C. roseus*-AgNPs treatment in HepG2 cells relative to THLE-3 cells.
 - d. To examine the morphological changes in HepG2 and THLE-3 cells after treatment compared to untreated cells.
2. To determine the oxidative stress effects induced by *C. roseus*-AgNPs in HepG2 and cells
 - a. To measure the nitric oxide production levels in HepG2 cells treated with *C. roseus*-AgNPs.
 - b. To explore the role of oxidative stress by assessing ROS levels in *C. roseus*-AgNPs-treated HepG2 cells.
 - c. To monitor intracellular calcium levels in HepG2 cells following treatment with *C. roseus*-AgNPs.
 - d. To observe changes in mitochondrial membrane potential in HepG2 cells treated with *C. roseus*-AgNPs.

3. To determine the mechanisms of cell death induced by *C. roseus*-AgNPs in HepG2 cells
 - a. To evaluate the activation of initiator caspases (caspase 8 for the extrinsic pathway and caspase 9 for the intrinsic pathway) and effector caspases (caspase 3/7) in *C. roseus*-AgNPs-treated HepG2 cells.
 - b. To analyse the cell cycle arrest induced by *C. roseus*-AgNPs in HepG2 cells.
 - c. To determine the mode of cell death in HepG2 cells treated with *C. roseus*-AgNPs.
 - d. To assess the effectiveness of *C. roseus*-AgNPs in inducing DNA damage in HepG2 cells.

4. To investigate the cellular uptake and intracellular distribution of *C. roseus*-AgNPs in HepG2 cells
 - a. To quantify the uptake of *C. roseus*-AgNPs by HepG2 cells.
 - b. To measure the exocytosis of *C. roseus*-AgNPs from HepG2 cells.
 - c. To identify the cellular uptake mechanisms of *C. roseus*-AgNPs using selective inhibitors.
 - d. To visualise the processes of uptake and exocytosis of *C. roseus*-AgNPs in HepG2 cells.

5. To assess the mRNA transcriptome profiling of *C. roseus*-AgNPs treated HepG2 cells
 - a. To isolate total RNA from HepG2 cells treated with *C. roseus*-AgNPs.

- b. To analyse differential gene expression between untreated and *C. roseus*-AgNPs-treated HepG2 cells.
- c. To investigate the molecular pathways activated in HepG2 cells following *C. roseus*-AgNPs treatment.

CHAPTER 2

LITERATURE REVIEW

2.1 Cancer

Cancer is a complex disease that arises from the accumulation of genetic abnormalities and epigenetic alterations in a cell, resulting in uncontrolled growth and division of aberrant cells (Mousavi *et al.*, 2018). A range of variables, including exposure to environmental toxins such as tobacco smoke, certain chemicals, and pollution, can create mutations in genes that can lead to cancer (Choi *et al.*, 2014). Ionising radiation, such as that emitted by X-rays or radioactive materials, can also result in mutations that lead to the development of cancer. Furthermore, certain viruses, such as the human papillomavirus (HPV) and the hepatitis B and C viruses, can induce infections that result in genetic changes in cells, raising the chance of developing certain types of cancer. Other risk factors for cancer include lifestyle factors such as diet and physical activity, as well as inherited genetic abnormalities that can raise the chance of cancer (Hudnall *et al.*, 2014).

Untargeted cells in the body have regulatory mechanisms that control their growth and division, preventing them from dividing indefinitely. However, cancer cells are preceded by the appearance of mutations in untargeted cells that disrupt these control mechanisms, allowing them to continue dividing and growing uncontrollably (Andleeb *et al.*, 2021). This is the initial stage of cancer development called initiation. As the mutated cells continue to proliferate (promotion), they can form a mass of a targeted cells called a tumour. Tumours can be benign, meaning they are not cancerous and do not spread to other parts of the body, or they can be malignant, meaning they are cancerous and can metastasis surrounding tissues and spread to other parts of the body through the bloodstream or lymphatic system (Sarkar *et al.*, 2013).

Cancer is a heterogeneous disease, meaning that it can have many different subtypes and genetic alterations that affect its behavior and response to treatment (Rivenbark *et al.*, 2013). The diagnosis and treatment of cancer are based on a combination of factors, including the type and stage of the cancer, the patient's age and overall health, and the presence of any other medical conditions (Yildizhan *et al.*, 2018). Treatment options can include surgery, chemotherapy, radiation therapy, immunotherapy, and targeted therapy, among others.

2.1.1 Global cancer statistics

Cancer is the leading cause of death, and its occurrence is steadily increasing. In 2020, global cancer statistics showed that an estimated 19.3 million new cancer cases (18.1 million excluding nonmelanoma skin cancer) and around 10.0 million cancer deaths (9.9 million excluding nonmelanoma skin cancer). Figure 2.1 showed female breast cancer has surpassed lung cancer as the most commonly diagnosed cancer, with an expected 2.3 million new cases (11.7%), followed by lung (11.4%), colorectal (10.0 %), prostate (7.3%), and stomach (5.6%) cancers (Sung *et al.*, 2021). Lung cancer remained the top cause of cancer death with an estimated 1.8 million fatalities (18%), followed by colorectal (9.4%), liver (8.3%), stomach (7.7%), and female breast (6.9%) cancers (Sung *et al.*, 2021).

In general, the occurrence of cancer was 2 to 3 times higher in countries that had completed their transition to modernisation compared to those in the midst of transitioning, for both males and females. However, whereas male mortality varied 2-fold, but female mortality varied little. Nonetheless, transitioning countries had much higher rates of breast and cervical cancer deaths among women compared to transitioned countries. Looking forward to 2040, the global burden of cancer is predicted to increase by 47%, totaling 28.4 million cases, with transitioning countries

facing a greater increase of 64% to 95% compared to 32% to 56% in transitioned countries. This rise is due to demographic shifts, the growing economy, and rising risk factors associated with globalisation. To improve global cancer control, it is necessary to create sustainable infrastructure to spread cancer prevention strategies and offer cancer care in transitioning nations (Sung *et al.*, 2021).

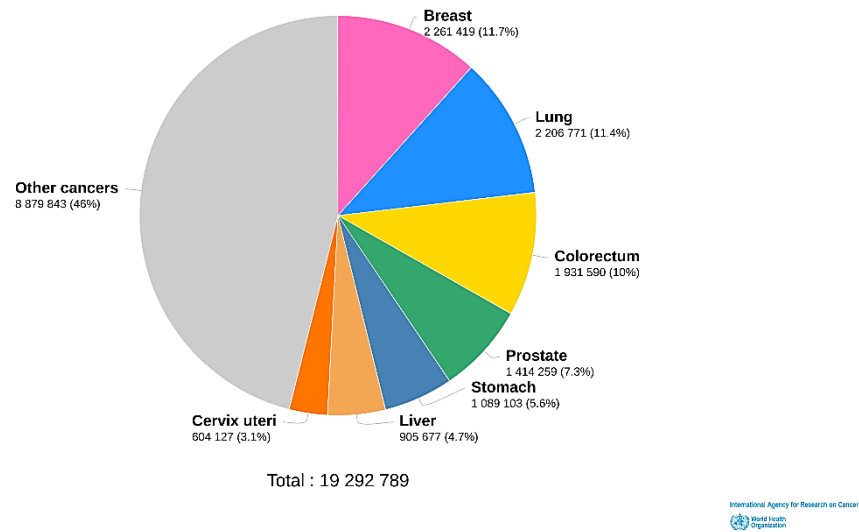


Figure 2.1 Estimated number of new cases worldwide in 2020. Taken from <http://gco.iarc.fr>

2.1.2 Cancer statistics in Malaysia

In 2020, Malaysia reported 48,639 new cases of cancer and this number indicates a steady increase in cancer incidence in the country. Alarming, cancer incidence in Malaysia is expected to double by 2040, which is a cause for concern (Schliemann *et al.*, 2020). Based on current statistics, approximately 1 in 10 people in Malaysia will be diagnosed with cancer during their lifetime. This means that the lifetime risk of developing cancer in Malaysia is 1 in 10 for males and 1 in 9 for females. Lifetime risk refers to the probability of a person developing cancer before the age of 75 years in the absence of other causes of death. As shown in Figure 2.2,

the top five most common cancers in Malaysia in 2020 were breast cancer (17.3%), followed with colorectal cancer (13.6%), lung cancer (10.6%), nasopharyngeal cancer (4.6%) and lastly, liver cancer (4.4%)(Schliemann *et al.*, 2020) . Lifestyle factors such as smoking, alcohol consumption, unhealthy diet, and lack of physical activity are believed to contribute to the increasing incidence of cancer in Malaysia (Schliemann *et al.*, 2020). To address this growing issue, the Malaysian government has implemented various initiatives to improve cancer care and access to treatment. These include establishing cancer centers and support groups, introducing a National Strategic Plan for Cancer Control Programme (NSPCCP) 2021-2025.

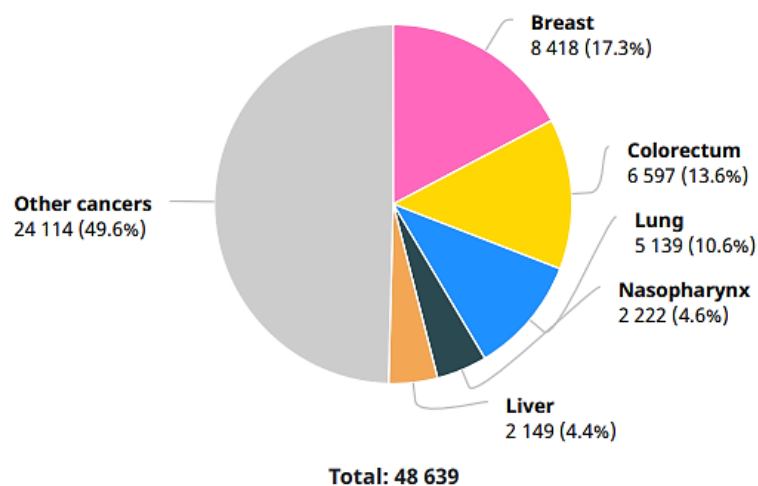


Figure 2.2 Number of new cases and the top common cancer in Malaysia in 2022. Taken from <http://gco.iarc.fr>

2.1.3 Hepatocellular carcinoma

Liver cancer is a significant health concern globally, including in Malaysia. According to the Global Cancer Observatory (Globocan) 2020, liver cancer is the sixth most common cancer among males in Malaysia, accounting for 6.7% of all new cancer cases in this group. It is also the third leading cause of cancer-related deaths in the country, contributing to 6.9% of all cancer deaths. Hepatocellular carcinoma (HCC) is the most common primary liver cancer and arises from the hepatocytes, which are the main functional cells of the liver (Bosch *et al.*, 2004). HCC accounts for up to 90% of all primary hepatic malignancies with nearly one million new cases diagnosed annually worldwide, HCC comprises a significant portion of the global cancer burden. The worldwide incidence of HCC with a predominant number of cases 72% occurring in Asia, of which over 50% are reported in China. The remaining HCC cases are distributed as follows: 10% in Europe, 7.8% in Africa, 5.1% in North America, 4.6% in Latin America, and 0.5% in Oceania (Ramai *et al.*, 2022)..

The factors that have been identified as risk factors for HCC development include chronic infection with hepatitis B or C viruses, heavy alcohol consumption, non-alcoholic fatty liver disease (NAFLD) or non-alcoholic steatohepatitis (NASH), and cirrhosis (Boyle *et al.*, 2017). People with chronic hepatitis B or C are at an increased risk of developing HCC as these viruses can cause liver inflammation and scarring over time (Abdualmjid *et al.*, 2022). Drinking large amounts of alcohol over a long period of time can also cause liver damage and increase the risk of liver cancer. Additionally, NAFLD and NASH, characterised by the build-up of fat in the liver, can cause liver inflammation and scarring, thereby increasing the risk of HCC. Cirrhosis, a chronic liver disease characterised by scarring of the liver, is also associated with an increased risk of HCC (Golabi *et al.*, 2017).

The prognosis for HCC varies depending on the stage of the disease at diagnosis, with early-stage tumours having a better prognosis than advanced-stage tumours (Wan *et al.*, 2022). To ensure the best possible treatment outcome for patients with HCC, a team of healthcare professionals with diverse expertise must make clinical decisions considering the patient's tumour stage, liver function, and performance status (Ramai *et al.*, 2022). Surgery is considered the best option if the cancer is confined to a specific area of the liver, but it may not be possible for patients with advanced disease or underlying medical conditions. Liver transplant is an option for patients with cirrhosis or liver failure, but it largely depends on finding a suitable donor liver and the patient's overall health (Llovet *et al.*, 2021). Other treatment options include ablation therapy, radiation therapy, and chemotherapy, which can be given orally or intravenously and may be used in combination with other treatments (Alqahtani *et al.*, 2019). However, these treatments have several limitations, including tumour recurrence, side effects such as fatigue and nausea, and limited effectiveness, especially in patients with advanced disease. In such cases, palliative care may be necessary to relieve symptoms and improve the patient's quality of life (Henson *et al.*, 2020).

2.2 Nanotechnology

2.2.1 Introduction

Nano is derived from the Greek word “nanos”, meaning dwarf, tiny, or very small (Rai *et al.*, 2008). Nanotechnology is a field of science and technology that focuses on manipulating and engineering materials at the atomic, molecular, and supramolecular scale, typically ranging from 1 to 100 nanometres (nm) (Ferrari *et al.*,

2005). Nanotechnology has the potential to revolutionise a wide range of industries, including medicine, electronics, energy, and materials science (Emerich *et al.*, 2005). Understanding the physicochemical properties of materials at the nanoscale will be essential in order to materialise the potential and develop new materials with novel features and functionalities that may be used for human well-being (Alexis *et al.*, 2008).

Nanobiotechnology emerged due to the application of nanotechnology in biotechnology, which was inevitable given the presence of naturally occurring nanoscale structures in living cells, which refers to the application of nanotechnology in the life sciences (Jain *et al.*, 2010). Nanomedicine is an application of nanobiotechnology that offers numerous potential medical applications, including developing new materials and devices that may interact with biological systems at the nanoscale. Some key focus areas in nanomedicine include drug and gene delivery, imaging agent, probing of DNA structure, tissue engineering, detection of pathogens, and phagokinetic (Foroozandeh *et al.*, 2018). Nanooncology is a rapidly growing field within nanomedicine that focuses on using nanotechnology for the diagnosis, imaging, and treatment of cancer (Jain *et al.*, 2010). Some examples of nanooncology applications are using quantum dots, gold nanoparticles conjugated with a monoclonal antibody, nanobiosensors to detect multiple molecular biomarkers of cancer, and nanocarrier magnetic and target delivery of drugs to the cancerous site (Choi *et al.*, 2006).

2.2.2 Biomedical Application of Nanomaterials

Nanomaterials exhibit unique properties and tremendous applicability, making them well-suited for medical applications (Silva *et al.*, 2004). One important aspect of nanomaterials is their high surface area-to-volume ratio, which can contribute to higher

reactivity, specificity, and adsorption capacity. This characteristic is extremely important in medical applications, as nanomaterials can be engineered to transport other compounds, such as probes, proteins, and drugs, to specified sites in the body (Zhang *et al.*, 2019). Another critical property of nanomaterials is their quantum properties, which can arise due to their small size. Some nanoparticles can exhibit fluorescent or magnetic properties that can be exploited in medical imaging or drug delivery applications (Silva *et al.*, 2004). Table 2.1 shows various types and structures of nanomaterials used in biomedical applications.

Table 2.1 Commonly used nanomaterials in biomedicine for various applications. Taken from Barkalina *et al.*(2014)

Class	Subclass	Material	Structure	Description		
Organic	Lipids	Phospholipids	Liposomes	Enclosed nanospheres comprised of a phospholipid bilayer		
			Micelles	Enclosed nanospheres comprised of a phospholipid monolayer		
		Solid lipids	Solid lipid nanoparticles	Nanospheres comprised of the lipid core stabilised by surfactants and/or polymers		
	Polymers	Poly-L-lactide-co-glycolide (PLGA) Poly-L-lactic acid (PLA) Chitosan Gelatine	Nanoparticles	Variously shaped structures with all three physical dimensions on the nanoscale (b 100 nm)		
			Polyamidoamine(PAMAM) Polypropyleneimine (PPI)	Dendrimers	Spherical nanomolecules consisting of the central core and sequential layers of branching groups	
Inorganic	Noble metals	Gold Silver Platinum	Nanoparticles	Variously shaped structures with all three physical dimensions on the nanoscale (b 100 nm)		
			Oxides	Magnetic and superparamagnetic iron oxides	Nanoparticles	Variously shaped structures with all three physical dimensions on the nanoscale (b 100 nm)
					Semiconductors	Cadmium Selenium Tellurium Indium
	Carbon-based	Carbon	Fullerenes	Hollow nanospheres, comprised of carbon atoms, forming cage-like structures		
			Nanotubes	Cylindrical structures with two of the three physical dimensions on		

Other	Mesoporous silica	Nanoparticles	the nanoscale (b 100 nm) Variously shaped structures with all three physical dimensions on the nanoscale (b 100 nm) and mesoporous architecture (Pore diameter: 2-50 nm)
-------	-------------------	---------------	--------------------------------------------------------------------------------------------------------------------------------------------------------------------------------

The use of nanomaterials in biomedical applications has tremendous potential for improving disease diagnosis and treatment, and is an area of active research and development, however, it is essential to note that using nanomaterials in medicine raises concerns about their potential toxicity and environmental impact. As such, researchers in nanotechnology are working to develop safe and sustainable methods for using nanomaterials in medical applications.

2.2.3 Clinically approved nanoparticles

Several types of nanoparticles formulations have been approved for use in cancer treatment by regulatory organisations such as the U.S. Food and Drug Administration (FDA). These nanoparticle formulations are designed to target cancer cells specifically while minimising toxicity to healthy cells.

Abraxane is one of the FDA approved nanoformulated drugs, which is a nanoparticle-bound form of the chemotherapy drug paclitaxel. Abraxane is used to treat breast cancer, non-small cell lung cancer, and pancreatic cancer. The nanoparticle-bound paclitaxel allows for increased drug delivery to cancer cells, resulting in higher efficacy and fewer side effects (Ventola *et al.*, 2017). Another example is Doxil, which is a liposomal formulation of the chemotherapy drug doxorubicin. Doxil is used to treat ovarian and breast cancers. The liposomal formulation allows for sustained drug release and increased accumulation of the drug in cancer cells (Min *et al.*, 2015). Table 2.2 illustrates several nanoparticle-based therapies in clinical trials for various types of cancer. Many clinically certified nanoparticle formulations used in cancer treatment are designed to target cancer cells passively by using the unique properties of nanoparticles rather than actively targeting

them by modifying nanoparticles using chemical-based targeting moieties (Zhang *et al.*, 2014). Active targeting has several advantages over passive targeting, including increased specificity and selectivity, improved drug delivery to the target site, and reduced toxicity to healthy tissues. Many clinically approved nanoparticle formulations still use passive targeting due to several reasons including the complexity and cost of developing and manufacturing active-targeted nanoparticles, the potential for off-target effects and toxicity, and the need for more extensive preclinical and clinical testing to demonstrate safety and efficacy (Anselmo and Mitragotri, 2016).

Table 2.2 Clinically approved intravenous nanoparticle therapies and diagnostics, grouped by their broad indication. Taken from Anselmo & Mitragotri (2016)

Name	Particle type/drug	Approved application/indication	Approval(year)	Investigated application/indication	ClinicalTrials.gov identifier
Doxil/Caelyx (Janssen)	Liposomal doxorubicin (PEGylated)	Ovarian cancer (secondary to platinum-based therapies) HIV-associated Kaposi's sarcoma (secondary to chemotherapy) Multiple myeloma (secondary)	FDA (1995) EMA (1996)	Various cancers including solid malignancies, ovarian, breast, leukemia, lymphomas, prostate, metastatic, or liver	166 studies mention Doxil 90 studies mention CAELYX
DaunoXome (Galen)	Liposomal daunorubicin (non-PEGylated)	HIV-associated Kaposi's sarcoma (primary)	FDA (1996)	Various leukemias	32 studies mention DaunoXome
Myocet (Teva UK)	Liposomal doxorubicin (non-PEGylated)	Treatment of metastatic breast cancer (primary)	EMA (2000)	Various cancers including breast, lymphoma, or ovarian.	32 studies mention Myocet
Abraxane (Celgene)	Albumin-particle bound paclitaxel	Advanced non-small cell lung cancer (surgery or radiation is not an option) Metastatic breast cancer (secondary) Metastatic pancreatic cancer (primary)	FDA (2005) EMA (2008)	Various cancers including: solid malignancies, breast, lymphomas, bladder, lung, pancreatic, head and neck, prostate, melanoma, or liver	295 studies mention Abraxane
Marqibo (Spectrum)	Liposomal vincristine (non-PEGylated)	Philadelphia chromosome-negative acute lymphoblastic leukemia (tertiary)	FDA (2012)	Various cancers including: lymphoma, brain, leukemia, or melanoma	23 studies mention Marqibo
MEPACT (Millennium)	Liposomal mifamurtide (non-PEGylated)	Treatment for osteosarcoma (primary following surgery)	EMA (2009)	Osteosarcomas	4 studies mention MEPACT: 3 active/recruiting
Onivyde MM-398 (Merrimack)	Liposomal irinotecan (PEGylated)	Metastatic pancreatic cancer (secondary)	FDA (2015)	Various cancers including: solid malignancies, breast, pancreatic, sarcomas, or brain	7 studies mention MM-398/Onivyde: 6 active/recruiting

2.3 Silver Nanoparticles (AgNPs)

2.3.1 Introduction

Silver nanoparticles (AgNPs) are a crucial and captivating type of nanomaterial that is widely used in the field of biomedicine, alongside other metallic nanoparticles. AgNPs have a significant impact on nanoscience and nanotechnology, particularly in the area of nanomedicine (Solati *et al.*, 2015). AgNPs exhibit unique properties at the nanoscale, such as a high surface area-to-volume ratio and surface modification properties, which make them attractive for use in medical applications. The small size of AgNPs allows for enhanced permeability and retention in tissues, which can increase their therapeutic efficacy. Additionally, AgNPs have intrinsic cytotoxic features due to the release of silver ions. As a result, AgNPs can be thought of as a two-in-one medicinal solution, such as antimicrobial, anti-inflammatory, and anticancer effects (Iravani *et al.*, 2014b). These AgNPs are being extensively studied for their potential use in a wide range of medical applications, including wound healing, drug delivery, diagnostic imaging, and cancer treatment. Other biological activities of AgNPs have been also explored, including promoting bone healing and wound repair, enhancing the immunogenicity of vaccines, and anti-diabetic effects (Xu *et al.*, 2020). The inherent properties of AgNPs, such as their size, shape, and surface charge play an efficient role in combating a diverse range of cancers, both in vitro and in vivo. These cancers include cervical cancer, breast cancer, lung cancer, hepatocellular carcinoma, nasopharyngeal carcinoma, glioblastoma, colorectal adenocarcinoma, and prostate carcinoma (Dyal *et al.*, 2006; Sukirtha *et al.*, 2012; Prabhu *et al.*, 2013; Liu, *et al.*, 2016).

2.3.2 Patent analysis of AgNPs in cancer therapy

Patent analysis of AgNPs in cancer therapy involves examining patents related to the use of AgNPs in the diagnosis, treatment, and monitoring of cancer. AgNPs have been explored as a potential tool in cancer therapy due to their unique physical and chemical properties, including their ability to penetrate cancer cells, generate reactive oxygen species, and exhibit localised surface plasmon resonance.

Patent analysis can also provide insights into the regulatory landscape for AgNP-based cancer therapies. For example, if a large number of patents are being filed for AgNP-based targeted drug delivery systems, it may suggest that there is a strong need and demand for such products, and that regulatory bodies may need to develop guidelines for their safe and effective use (Lens, 2022).

Based on Figure 2.3, the patent documents related to AgNPs in cancer therapy that were published, filed, and granted showed an increasing trend up to 2022. This trend indicates a growing interest and investment in AgNPs-based cancer therapies and suggests that researchers and companies recognise the potential of AgNPs in cancer diagnosis, treatment, and monitoring. The increasing number of patent documents also reflects the competitive landscape in the field, as more companies and research groups seek to protect their intellectual property and secure a market share in the rapidly growing field of AgNP-based cancer therapy. The trend also highlights the need for continued innovation and development in the field, as stakeholders seek to improve the safety and efficacy of AgNPs-based cancer therapies and address challenges such as regulatory approval and clinical translation.

Overall, the increasing trend of patent documents related to AgNPs in cancer therapy demonstrates the importance and potential of this field and highlights the need

for continued investment and collaboration to drive innovation and improve patient outcomes.

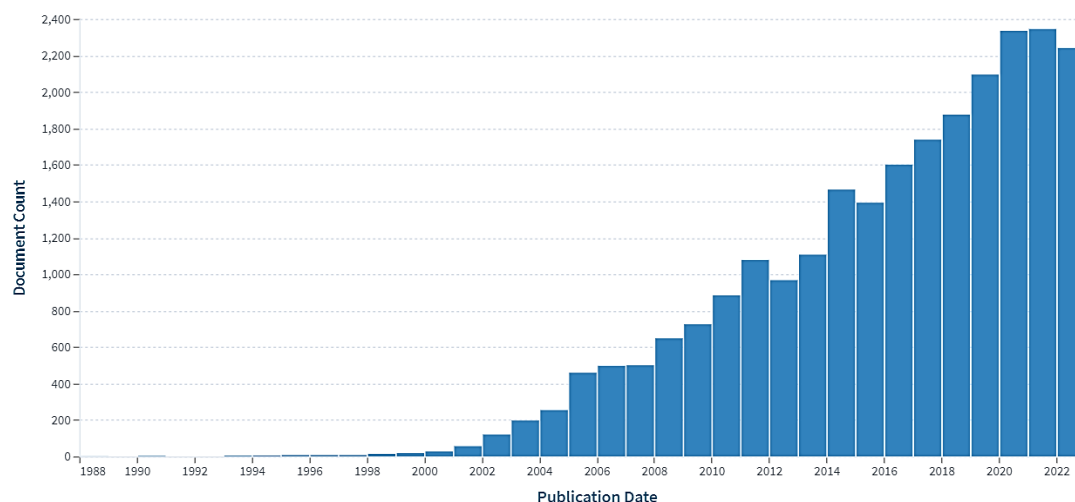


Figure 2.3 The patent documents related to AgNPs in cancer therapy that were published, filed, and granted over the years. Taken from Lens.org

2.3.3 Synthesis of AgNPs

The synthesis methods of AgNPs can be broadly classified into two categories into two processes which were top-down and bottom-up as shown in Figure 2.4.

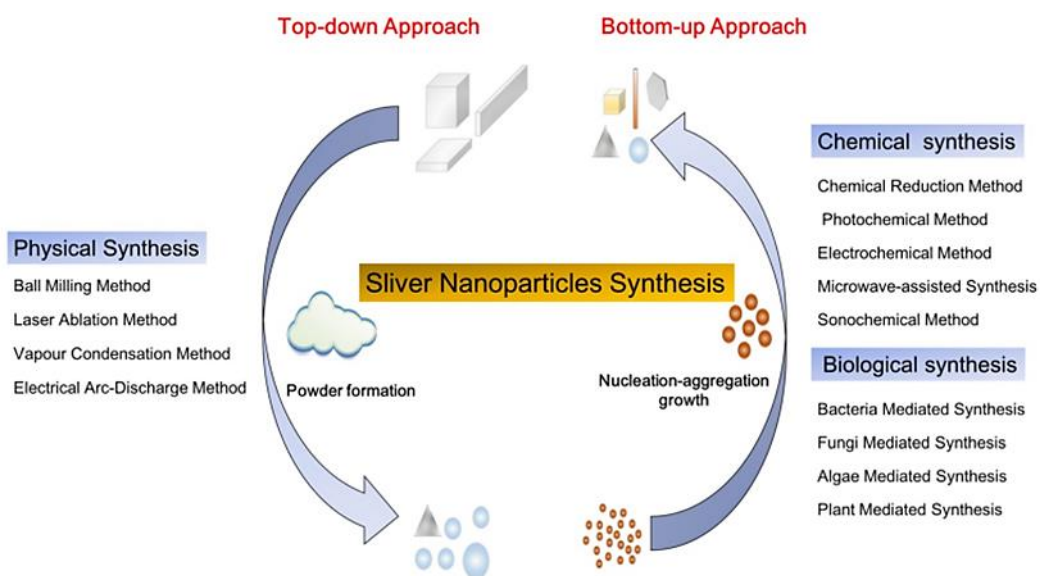


Figure 2.4 AgNPs synthesis top-down approach and bottom-up approach. Taken from Xu *et al.* (2020)